Progress In Electromagnetics Research, PIER 30, 85–104, 2001

SPACE-HARMONIC EFFECTS IN HELICAL SLOW-WAVE STRUCTURE — AN EQUIVALENT CIRCUIT ANALYSIS

S. Ghosh, A. K. Sinha, R. K. Gupta, and S. N. Joshi

Central Electronics Engineering Research Institute
Pilani, Rajasthan 333 031, India

P. K. Jain and B. N. Basu

Centre of Research in Microwave Tubes
Department of Electronics Engineering
Institute of Technology, Banaras Hindu University
Varanasi 221 005, India

Abstract–The analysis of a lossless helical slow-wave structure (SWS) using equivalent circuit approach, reported elsewhere, had been carried out for the fundamental mode only. This is essentially used to predict the transmission line parameters. Moreover, in the analysis the effect of permittivity on the radial propagation constant has not been considered. The radial propagation constant was considered to be same over the different structure regions. In this paper, the analysis has been developed for the space-harmonic modes considering different radial propagation constant over different structure regions. Due to it, the present analysis becomes more general, accurate and capable of dealing with a wide range of structure parameters. The dispersion relation developed here in terms of the equivalent line parameters for a lossless structure, namely, shunt capacitance per unit length and series inductance per unit length for the space-harmonic modes, as a special case, passes on to those obtained earlier by considering same radial propagation constants over different structure regions and for the fundamental mode. Besides the dispersion characteristics, characteristics impedance has also been predicted in terms of line parameters. The results presented here in terms of the structure parameters can be used for structure design and performance evaluation as well as for the control of any space harmonic of interest. The present analysis has also been validated with those experimental values reported elsewhere.

1. INTRODUCTION

The helix, a non-resonant electromagnetic structure, finds widest application both in civil and defence when used as a slow-wave structure (SWS) in a wideband traveling-wave tube (TWT). The performance characteristics of the helix, like, power, gain, bandwidth, etc. can be considerably improved by suitably tailoring its design and with the help of modern technological approaches.

In a practical TWT, helix is held in a position by a number of dielectric rods/bars symmetrically arranged around the helix and the whole is enclosed in a metal envelope. Such a support geometry essentially causes an inhomogeneous loading of the helix [1–6]. To analyse such an inhomogeneously loaded helical SWS, two analytical techniques are frequently used: the field analytical approach [1–6] and the equivalent circuit analytical approach [7–9]. However, both these analytical techniques yield one the same dispersion relation, the equivalent circuit analytical approach to be somewhat simple in that. In this approach, one has to handle at a time only half of the total number of the boundary conditions of the problem in order to obtain a line parameter — capacitance per unit length or inductance per unit length for a lossless structure [7] and thus reduces the complexity of the problem.

The equivalent circuit analysis, reported earlier [7–9], is for the homogeneously loaded helical SWS and handles only the fundamental mode of the space harmonic and also ignores the effect of inequality of the radial propagation constant. In this paper, a set of expressions for the equivalent transmission line parameters have been derived for an inhomogeneously loaded helix in the sheath model, for the mth mode of the space-harmonics [10–12], by considering non-uniformity of radial propagation constant over the structure regions [2], and use them to determine the dispersion characteristics of the structure to tailor the device bandwidth or to design space-harmonic devices of interest or to control the undesirable space-harmonic modes. The present method which is simple, further extended to study another useful

parameter, namely, the characteristics impedance. However, the interaction impedance of the structure is out of scope from this present analysis. The analytical results presented here also pass on to those, reported elsewhere, as a special case, by considering same radial propagation constant and for the fundamental mode only [7–9]. Moreover, in the analytical results the effect of helix wire/tape thickness [13, 14] has been ignored but considered in the actual analysis. Finally, the results for the axial propagation constant of the fundamental mode has also been validated with those experimental values published in the literature [15].

2. ANALYSIS

For the analysis let us consider a helix supported by a number of identical discrete dielectric rods/bars of an arbitrary cross section in a metal envelope (Fig. 1a). Such a support geometry, in general, causes an inhomogeneous loading and may be analysed in a model in which the discrete supports are azimuthally smoothed out into n number of continuous dielectric tube regions of effective permittivity values — the value of n may be increased for the desired convergence accuracy [3] (Fig. 1b). Considering the rf quantities associated with the mth mode to vary as $\exp j(\psi t - \beta_m z + m\theta)$, one may write the following expressions for the components of the electric (E) and magnetic (H) field intensities in the different regions of the structure in the cylindrical co-ordinate (r, θ, z) system for the mth mode in sheath-helix model [10, 13]:

$$
\begin{aligned}
E_{z,m,p} &= \left[A_{m,p} I_m\{\gamma_{m,p} r\} + B_{m,p} K_m\{\gamma_{m,p} r\}\right], \\
H_{z,m,p} &= \left[C_{m,p} I_m\{\gamma_{m,p} r\} + D_{m,p} K_m\{\gamma_{m,p} r\}\right], \\
E_{\theta,m,p} &= -\left[\left(\frac{m\beta_m}{r\gamma_{m,p}^2}\right)\left(A_{m,p} I_m\{\gamma_{m,p} r\} + B_{m,p} K_m\{\gamma_{m,p} r\}\right)\right. \\
&\quad \left. + \left(\frac{j\omega\mu_0}{\gamma_{m,p}}\right)\left(C_{m,p} I'_m\{\gamma_{m,p} r\} + D_{m,p} K'_m\{\gamma_{m,p} r\}\right)\right], \\
H_{\theta,m,p} &= \left[\left(\frac{j\omega\varepsilon_0\varepsilon'_{r,p}}{\gamma_{m,p}}\right)\left(A_{m,p} I'_m\{\gamma_{m,p} r\} + B_{m,p} K'_m\{\gamma_{m,p} r\}\right)\right. \\
&\quad \left. - \left(\frac{m\beta_m}{r\gamma_{m,p}^2}\right)\left(C_{m,p} I_m\{\gamma_{m,p} r\} + D_{m,p} K_m\{\gamma_{m,p} r\}\right)\right],
\end{aligned}
$$

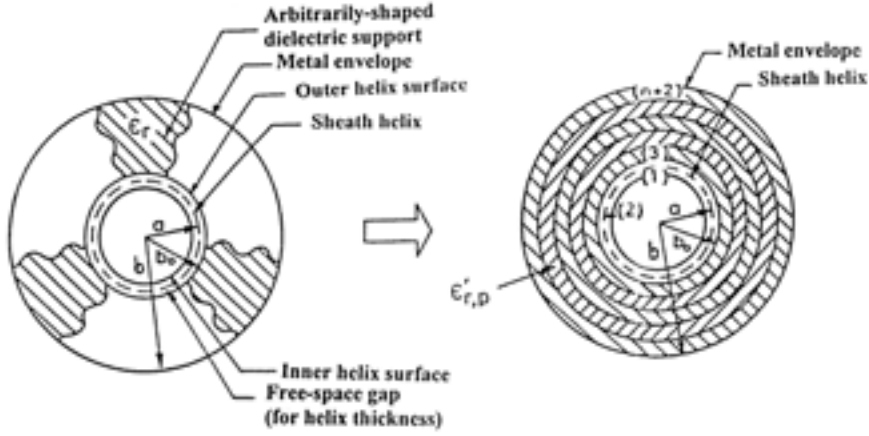

Figure 1. Cross section of an inhomogeneously loaded helix supported by (a) arbitrarily-shaped dielectric bars and (b) its equivalent analytical model.

$$E_{r,m,p} = \left[\left(\frac{j\beta_m}{\gamma_{m,p}}\right)\left(A_{m,p}I'_m\{\gamma_{m,p}r\} + B_{m,p}K'_m\{\gamma_{m,p}r\}\right) - \left(\frac{m\omega\mu_0}{r\gamma^2_{m,p}}\right)\left(C_{m,p}I_m\{\gamma_{m,p}r\} + D_{m,p}K_m\{\gamma_{m,p}r\}\right)\right]$$

and

$$H_{r,m,p} = \left[\left(\frac{m\omega\varepsilon_0\varepsilon'_{r,p}}{r\gamma^2_{m,p}}\right)\left(A_{m,p}I_m\{\gamma_{m,p}r\} + B_{m,p}K_m\{\gamma_{m,p}r\}\right) + \left(\frac{j\beta_m}{\gamma_{m,p}}\right)\left(C_{m,p}I'_m\{\gamma_{m,p}r\} + D_{m,p}K'_m\{\gamma_{m,p}r\}\right)\right], \quad (1)$$

where p refers to a region of the structure (Fig. 1b). $A_{m,p}$, $B_{m,p}$, $C_{m,p}$, and $D_{m,p}$ are the field constants. $\gamma_{m,p}$ $(= (\beta_m^2 - \varepsilon'_{r,p}k^2)^{1/2})$ is the radial propagation constant of pth region, k $(= \omega(\mu_0\varepsilon_0)^{1/2})$ and β_m $(= \beta_0 + m\cot\psi/a)$ being the free space and axial propagation constants of the structure, respectively. ψ and a are the pitch angle and the mean radius of the helix, respectively, and $\varepsilon'_{r,p}$ $(= 1 + (\varepsilon_r - 1)\hat{A}_{s,p}/\hat{A}_p)$ represents the effective relative permittivity [1–4] of the pth of the n effective dielectric tube regions into which the discrete supports are azimuthally smoothed out (Fig. 1), $\hat{A}_p$ being the cross-sectional area

of the entire pth tube, $\hat{A}_{s,p}$ the cross-sectional area of the actual discrete supports in the pth tube region, and ε_r the relative permittivity of the support material, m represents the mode of the sheath helix. $I_m\{\gamma_{m,p}r\}$ and $K_m\{\gamma_{m,p}r\}$ represent the modified Bessel functions of order m of the first and second kinds, respectively, the prime indicating their derivative with respect to the argument.

In the analytical model, considered here, has $n+2$ regions (Fig. 1b): the free-space region $(p=1,\ \varepsilon'_{r,1}=1,\ 0\le r\le a)$ inside the winding radius $(r=a)$ of the helical sheath, the free- space gap $(p=2,\ \varepsilon'_{r,2}=1,\ a\le r\le b_0)$ between the sheath and the beginning $(r=b_0)$ of the dielectric regions, to take into account the finite helix wire/tape thickness [13, 14] $(=2(b_0-a))$, and n dielectric tube regions. Out of $(4n+8)$ field constants relevant to these $(n+2)$ regions, $B_{m,1}$ and $D_{m,1}$ become equal to zero to satisfy the condition that the fields are to be finite at the axis $(r=0)$ of the structure, giving $(4n+6)$ non-zero field constants. The relevant boundary conditions for the problem are: (i) the sheath helix boundary conditions, at $r=a$ [11], (ii) the boundary conditions related to the continuity of the tangential components of the electric and magnetic field intensities at each of the interfaces $(r=b_p)$ between the discrete tube regions (between the pth and $(p+1)$th), and (iii) the boundary conditions that the tangential components of the electric field intensities are null at the metallic boundary $(r=b_n=b)$. With the help of the boundary conditions, the remaining $(4n+6)$ field constants can be grouped into two: one comprising of $A_{m,p}$ and $B_{m,p}$ — expressed in terms of a single constant, namely, $A_{m,1}$ and the other of $C_{m,p}$ and $D_{m,p}$ — expressed in terms of a single constant, namely, $C_{m,1}$. Using the sets of boundary conditions at the sheath helix $(r=a)$, one may express $A_{m,1}$ and $C_{m,1}$ in terms of I_{za} and $I_{\theta a}$, the axial and azimuthal components of sheath-helix current, respectively. The axial and azimuthal electric fields at the sheath helix $(r=a)$ are then expressed in terms of $A_{m,1}$ and $C_{m,1}$, respectively, and hence in terms of I_{za} and $I_{\theta a}$, respectively. These field expressions can now be converted into the transmission line equations, from which, one can get the expressions for the capacitance per unit length $C_{e,m}$ and inductance per unit length $L_{e,m}$ of the structure after a lengthy algebraic formulations as [10] (Appendix A):

$$C_{e,m}=C_{0,m}\alpha_{c,m}, \tag{2}$$

and

$$L_{e,m} = L_{0,m}\alpha_{1,m}. \tag{3}$$

Where $C_{0,m}$ and $L_{0,m}$ occurring in (2) and (3), respectively, are the expressions for the transmission line parameters of the mth mode of the space-harmonics for a helix in free- space and are given as:

$$C_{0,m} = \left(\frac{2\pi\beta_m\varepsilon_0}{\gamma_m^2}\right)\left(\frac{\left(\gamma_m^2 a + m^2\right)\cot\psi}{m + a\beta_m\cot\psi}\right)\left(1 - \frac{m\beta_m\cot\psi}{\gamma_m^2 a}\right)^{-1} \cdot \left(I_m\{\gamma_m a\}K_m\{\gamma_m a\}\right)^{-1}, \tag{4}$$

$$L_{0,m} = -\left(\frac{\beta_m\mu_0\cot^2\psi}{2\pi}\right)\left(\frac{\left(\gamma_m^2 a + m^2\right)\cot\psi}{m + a\beta_m\cot\psi}\right)^{-1}\left(1 - \frac{m\beta_m\cot\psi}{\gamma_m^2 a}\right)^{-1} \cdot I'_m\{\gamma_m a\}K'_m\{\gamma_m a\}, \tag{5}$$

and $\alpha_{c,m}$, $\alpha_{1,m}$ are the functions of structure parameters, and are given as:

$$\alpha_{c,m} = \left(1 + \frac{P_{m,0}I_m\{\gamma_m a\}}{Q_{m,0}K_m\{\gamma_m a\}}\right)^{-1}, \tag{6}$$

$$\alpha_{1,m} = \left(1 + \frac{S_{m,0}I'_m\{\gamma_m a\}}{R_{m,0}K'_m\{\gamma_m a\}}\right), \tag{7}$$

Where $\gamma_m\ (= \gamma_{m,1} = \gamma_{m,2}) = (\beta_m^2 - k^2)^{-1/2}$ is the radial propagation constant of the free-space region $0 \le r \le a$ and $a \le r \le b_0$. $P_{m,0}$, $Q_{m,0}$, $R_{m,0}$, and $S_{m,0}$ are given by:
For $2 \le p \le n$

$$\begin{aligned} P_{m,p-2} = &\left[\left(\varepsilon'_{r,p}\frac{K_m\{\gamma_{m,p+1}b_{p-2}\}}{I_m\{\gamma_{m,p}b_{p-2}\}} - \frac{\gamma_{m,p}}{\gamma_{m,p+1}}\varepsilon'_{r,p+1}\frac{K'_m\{\gamma_{m,p+1}b_{p-2}\}}{I'_m\{\gamma_{m,p}b_{p-2}\}}\right)P_{m,p-1}\right. \\ &+\left(\varepsilon'_{r,p}\frac{I_m\{\gamma_{m,p+1}b_{p-2}\}}{I_m\{\gamma_{m,p}b_{p-2}\}} - \frac{\gamma_{m,p}}{\gamma_{m,p+1}}\varepsilon'_{r,p+1}\frac{I'_m\{\gamma_{m,p+1}b_{p-2}\}}{I'_m\{\gamma_{m,p}b_{p-2}\}}\right)Q_{m,p-1} \\ &+\frac{m\beta_m}{\omega\varepsilon_0 b_{p-2}\gamma_{m,p}}\left(1 - \frac{\gamma_{m,p}^2}{\gamma_{m,p+1}^2}\right) \\ &\left.\cdot\left(\frac{R_{m,p-1}K_m\{\gamma_{m,p+1}b_{p-2}\} + S_{m,p-1}I_m\{\gamma_{m,p+1}b_{p-2}\}}{I'_m\{\gamma_{m,p}b_{p-2}\}}\right)\right] \\ &\cdot I_m\{\gamma_{m,p}b_{p-2}\}I'_m\{\gamma_{m,p}b_{p-2}\} \end{aligned} \tag{8}$$

$$
\begin{aligned}
Q_{m,p-2}=-\Bigg[&\left(\varepsilon'_{r,p}\frac{K_m\{\gamma_{m,p+1}b_{p-2}\}}{K_m\{\gamma_{m,p}b_{p-2}\}}-\frac{\gamma_{m,p}}{\gamma_{m,p+1}}\varepsilon'_{r,p+1}\frac{K'_m\{\gamma_{m,p+1}b_{p-2}\}}{K'_m\{\gamma_{m,p}b_{p-2}\}}\right)P_{m,p-1}\\
&+\left(\varepsilon'_{r,p}\frac{I_m\{\gamma_{m,p+1}b_{p-2}\}}{K_m\{\gamma_{m,p}b_{p-2}\}}-\frac{\gamma_{m,p}}{\gamma_{m,p+1}}\varepsilon'_{r,p+1}\frac{I'_m\{\gamma_{m,p+1}b_{p-2}\}}{K'_m\{\gamma_{m,p}b_{p-2}\}}\right)Q_{m,p-1}\\
&+\frac{m\beta_m}{\omega\varepsilon_0 b_{p-2}\gamma_{m,p}}\left(1-\frac{\gamma^2_{m,p}}{\gamma^2_{m,p+1}}\right)\\
&\cdot\left(\frac{R_{m,p-1}K_m\{\gamma_{m,p+1}b_{p-2}\}+S_{m,p-1}I_m\{\gamma_{m,p+1}b_{p-2}\}}{K'_m\{\gamma_{m,p}b_{p-2}\}}\right)\Bigg]\\
&\cdot K_m\{\gamma_{m,p}b_{p-2}\}K'_m\{\gamma_{m,p}b_{p-2}\} \qquad (9)\\
R_{m,p-2}=\Bigg[&\left(\frac{K_m\{\gamma_{m,p+1}b_{p-2}\}}{I_m\{\gamma_{m,p}b_{p-2}\}}-\frac{\gamma_{m,p}}{\gamma_{m,p+1}}\frac{K'_m\{\gamma_{m,p+1}b_{p-2}\}}{I'_m\{\gamma_{m,p}b_{p-2}\}}\right)R_{m,p-1}\\
&+\left(\frac{I_m\{\gamma_{m,p+1}b_{p-2}\}}{I_m\{\gamma_{m,p}b_{p-2}\}}-\frac{\gamma_{m,p}}{\gamma_{m,p+1}}\frac{I'_m\{\gamma_{m,p+1}b_{p-2}\}}{I'_m\{\gamma_{m,p}b_{p-2}\}}\right)S_{m,p-1}\\
&+\frac{m\beta_m}{\omega\mu_0 b_{p-2}\gamma_{m,p}}\left(1-\frac{\gamma^2_{m,p}}{\gamma^2_{m,p+1}}\right)\\
&\cdot\left(\frac{P_{m,p-1}K_m\{\gamma_{m,p+1}b_{p-2}\}+Q_{m,p-1}I_m\{\gamma_{m,p+1}b_{p-2}\}}{I'_m\{\gamma_{m,p}b_{p-2}\}}\right)\Bigg]\\
&\cdot I_m\{\gamma_{m,p}b_{p-2}\}I'_m\{\gamma_{m,p}b_{p-2}\} \qquad (10)
\end{aligned}
$$

and

$$
\begin{aligned}
S_{m,p-2}=-\Bigg[&\left(\frac{K_m\{\gamma_{m,p+1}b_{p-2}\}}{K_m\{\gamma_{m,p}b_{p-2}\}}-\frac{\gamma_{m,p}}{\gamma_{m,p+1}}\frac{K'_m\{\gamma_{m,p+1}b_{p-2}\}}{K'_m\{\gamma_{m,p}b_{p-2}\}}\right)R_{m,p-1}\\
&+\left(\frac{I_m\{\gamma_{m,p+1}b_{p-2}\}}{K_m\{\gamma_{m,p}b_{p-2}\}}-\frac{\gamma_{m,p}}{\gamma_{m,p+1}}\frac{I'_m\{\gamma_{m,p+1}b_{p-2}\}}{K'_m\{\gamma_{m,p}b_{p-2}\}}\right)S_{m,p-1}\\
&+\frac{m\beta_m}{\omega\mu_0 b_{p-2}\gamma_{m,p}}\left(1-\frac{\gamma^2_{m,p}}{\gamma^2_{m,p+1}}\right)\\
&\cdot\left(\frac{P_{m,p-1}K_m\{\gamma_{m,p+1}b_{p-2}\}+Q_{m,p-1}I_m\{\gamma_{m,p+1}b_{p-2}\}}{K'_m\{\gamma_{m,p}b_{p-2}\}}\right)\Bigg]\\
&\cdot K_m\{\gamma_{m,p}b_{p-2}\}K'_m\{\gamma_{m,p}b_{p-2}\} \qquad (11)
\end{aligned}
$$

where

$$
\begin{aligned}
P_{m,n-1} = {} & K_m\{\gamma_{m,n+2}b_{n-1}\}I_m\{\gamma_{m,n+1}b_{n-1}\} \\
& \cdot \left[\frac{\gamma_{m,n+1}}{\gamma_{m,n+2}}\varepsilon'_{r,n+2}\left(1-\frac{I'_m\{\gamma_{m,n+2}b_{n-1}\}K_m\{\gamma_{m,n+2}b\}}{K'_m\{\gamma_{m,n+2}b_{n-1}\}I_m\{\gamma_{m,n+2}b\}}\right)\right. \\
& \cdot \frac{K'_m\{\gamma_{m,n+2}b_{n-1}\}}{K_m\{\gamma_{m,n+2}b_{n-1}\}} - \varepsilon'_{r,n+1}\left(1-\frac{I_m\{\gamma_{m,n+2}b_{n-1}\}K_m\{\gamma_{m,n+2}b\}}{K_m\{\gamma_{m,n+2}b_{n-1}\}I_m\{\gamma_{m,n+2}b\}}\right) \\
& \cdot \frac{I'_m\{\gamma_{m,n+1}b_{n-1}\}}{I_m\{\gamma_{m,n+1}b_{n-1}\}} - \frac{m\beta_m\gamma_m(1-\gamma^2_{m,n+1}/\gamma^2_{m,n+2})}{\omega^2\mu_0\varepsilon_0\cot\psi\varepsilon'_{r,n+1}\varepsilon'_{r,n+1}b_{n-1}\gamma_{m,n+1}} \\
& \cdot \left(\frac{P_{m,0}K_m\{\gamma_m a\}+Q_{m,0}I_m\{\gamma_m a\}}{R_{m,0}K'_m\{\gamma_m a\}+S_{m,0}I'_m\{\gamma_m a\}}\right) \\
& \cdot \left.\left(1-\frac{I_m\{\gamma_{m,n+2}b_{n-1}\}K'_m\{\gamma_{m,n+2}b\}}{K_m\{\gamma_{m,n+2}b_{n-1}\}I'_m\{\gamma_{m,n+2}b\}}\right)\right] \qquad (12) \\
Q_{m,n-1} = {} & -K_m\{\gamma_{m,n+2}b_{n-1}\}K_m\{\gamma_{m,n+1}b_{n-1}\} \\
& \cdot \left[\frac{\gamma_{m,n+1}}{\gamma_{m,n+2}}\varepsilon'_{r,n+2}\left(1-\frac{I'_m\{\gamma_{m,n+2}b_{n-1}\}K_m\{\gamma_{m,n+2}b\}}{K'_m\{\gamma_{m,n+2}b_{n-1}\}I_m\{\gamma_{m,n+2}b\}}\right)\right. \\
& \cdot \frac{K'_m\{\gamma_{m,n+2}b_{n-1}\}}{K_m\{\gamma_{m,n+2}b_{n-1}\}} - \varepsilon'_{r,n+1}\left(1-\frac{I_m\{\gamma_{m,n+2}b_{n-1}\}K_m\{\gamma_{m,n+2}b\}}{K_m\{\gamma_{m,n+2}b_{n-1}\}I_m\{\gamma_{m,n+2}b\}}\right) \\
& \cdot \frac{K'_m\{\gamma_{m,n+1}b_{n-1}\}}{K_m\{\gamma_{m,n+1}b_{n-1}\}} - \frac{m\beta_m\gamma_m(1-\gamma^2_{m,n+1}/\gamma^2_{m,n+2})}{\omega^2\mu_0\varepsilon_0\cot\psi\varepsilon'_{r,n}\varepsilon'_{r,n+1}b_{n-1}\gamma_{m,n+1}} \\
& \cdot \left(\frac{P_{m,0}K_m\{\gamma_m a\}+Q_{m,0}I_m\{\gamma_m a\}}{R_{m,0}K'_m\{\gamma_m a\}+S_{m,0}I'_m\{\gamma_m a\}}\right) \\
& \cdot \left.\left(1-\frac{I_m\{\gamma_{m,n+2}b_{n-1}\}K'_m\{\gamma_{m,n+2}b\}}{K_m\{\gamma_{m,n+2}b_{n-1}\}I'_m\{\gamma_{m,n+2}b\}}\right)\right] \qquad (13) \\
R_{m,n-1} = {} & -K_m\{\gamma_{m,n+2}b_{n-1}\}I_m\{\gamma_{m,n+1}b_{n-1}\} \\
& \cdot \left[\frac{\gamma_{m,n+1}}{\gamma_{m,n+2}}\left(1-\frac{I'_m\{\gamma_{m,n+2}b_{n-1}\}K'_m\{\gamma_{m,n+2}b\}}{K'_m\{\gamma_{m,n+2}b_{n-1}\}I'_m\{\gamma_{m,n+2}b\}}\right)\right. \\
& \cdot \frac{K'_m\{\gamma_{m,n+2}b_{n-1}\}}{K_m\{\gamma_{m,n+2}b_{n-1}\}} - \left(1-\frac{I_m\{\gamma_{m,n+2}b_{n-1}\}K'_m\{\gamma_{m,n+2}b\}}{K_m\{\gamma_{m,n+2}b_{n-1}\}I'_m\{\gamma_{m,n+2}b\}}\right) \\
& \cdot \frac{I'_m\{\gamma_{m,n+1}b_{n-1}\}}{I_m\{\gamma_{m,n+1}b_{n-1}\}} - \frac{m\beta_m\varepsilon'_{r,n}\varepsilon'_{r,n+1}(1-\gamma^2_{m,n+1}/\gamma^2_{m,n+2})}{\gamma_m b_{n-1}\gamma_{m,n+1}} \\
& \cdot \left(\frac{R_{m,0}K'_m\{\gamma_m a\}+S_{m,0}I'_m\{\gamma_m a\}}{P_{m,0}K_m\{\gamma_m a\}+Q_{m,0}I_m\{\gamma_m a\}}\right) \\
& \cdot \left.\left(1-\frac{I_m\{\gamma_{m,n+2}b_{n-1}\}K_m\{\gamma_{m,n+2}b\}}{K_m\{\gamma_{m,n+2}b_{n-1}\}I_m\{\gamma_{m,n+2}b\}}\right)\right] \qquad (14)
\end{aligned}
$$

and

$$
\begin{aligned}
S_{m,n-1} = {} & K_m\{\gamma_{m,n+2}b_{n-1}\}K_m\{\gamma_{m,n+1}b_{n-1}\} \\
& \cdot \left[\frac{\gamma_{m,n+1}}{\gamma_{m,n+2}}\left(1 - \frac{I'_m\{\gamma_{m,n+2}b_{n-1}\}K'_m\{\gamma_{m,n+2}b\}}{K'_m\{\gamma_{m,n+2}b_{n-1}\}I'_m\{\gamma_{m,n+2}b\}}\right)\right. \\
& \cdot \frac{K'_m\{\gamma_{m,n+2}b_{n-1}\}}{K_m\{\gamma_{m,n+2}b_{n-1}\}} - \left(1 - \frac{I_m\{\gamma_{m,n+2}b_{n-1}\}K'_m\{\gamma_{m,n+2}b\}}{K_m\{\gamma_{m,n+2}b_{n-1}\}I'_m\{\gamma_{m,n+2}b\}}\right) \\
& \cdot \frac{K'_m\{\gamma_{m,n+1}b_{n-1}\}}{K_m\{\gamma_{m,n+1}b_{n-1}\}} - \frac{m\beta_m\varepsilon'_{r,n}\varepsilon'_{r,n+1}(1-\gamma^2_{m,n+1}/\gamma^2_{m,n+2})}{\gamma_m b_{n-1}\gamma_{m,n+1}} \\
& \cdot \left(\frac{R_{m,0}K'_m\{\gamma_m a\} + S_{m,0}I'_m\{\gamma_m a\}}{P_{m,0}K_m\{\gamma_m a\} + Q_{m,0}I_m\{\gamma_m a\}}\right) \\
& \left. \cdot \left(1 - \frac{I_m\{\gamma_{m,n+2}b_{n-1}\}K_m\{\gamma_{m,n+2}b\}}{K_m\{\gamma_{m,n+2}b_{n-1}\}I_m\{\gamma_{m,n+2}b\}}\right)\right]. \qquad (15)
\end{aligned}
$$

Once the expressions for the line parameters for a loss less structure, namely, $C_{e,m}$ and $L_{e,m}$ are obtained, the dispersion relation of the structure can be obtained from the transmission line equation as:

$$\beta_m^2 = \omega^2 L_{e,m} C_{e,m} \qquad (16)$$

Finally, by substituting (2) and (3) in (16) one gets the dispersion relation of the structure for the mth mode of the space-harmonics as follows:

$$
\begin{aligned}
& \left(1 - \frac{m\beta_m \cot\psi}{\gamma_m^2 a}\right)^2 (\alpha_{1,m}\alpha_{c,m})^{-1} I_m\{\gamma_m a\}K_m\{\gamma_m a\} \\
& + \left(\frac{k\cot\psi}{\gamma_m}\right)^2 I'_m\{\gamma_m a\}K'_m\{\gamma_m a\} = 0. \qquad (17)
\end{aligned}
$$

Similarly, the characteristics impedance $Z_{e,m}$ of the structure, can also be predicted as:

$$Z_{e,m} = (L_{e,m}/C_{e,m})^{0.5} \qquad (18)$$

The values of $L_{e,m}$ and $C_{e,m}$ are given in (3) and (4), respectively. The expressions for the interaction impedance [2–6] are out of scope here.

Special Case:

Here, it is of interest to mention that from the dispersion relation (17) — for an inhomogeneously loaded helix in the sheath-model, one

can get the same dispersion relation for an inhomogeneously loaded helix in the tape-model [2] without going through rigorous field analysis, by multiplying both sides of (17) by $\sin(\beta_n\delta/2)/(\beta_n\delta/2)$ and then summing up the equation from $-\propto$ to $+\propto$. Moreover, on substituting $\gamma_{m,1} = \gamma_{m,2} = \ldots = \gamma_{m,p} = \ldots = \gamma_{m,n+2} = \gamma_m$, and $m = 0$ (that is for the fundamental mode), the expressions for the line parameters (2) and (3) and hence the dispersion relation (17) passes on to those obtained earlier [8].

3. RESULTS AND DISCUSSION

It is of interest to study the effects of the various support parameters on the equivalent circuit parameters of the helical SWS, namely, the inductance per unit length $(L_{e,m})$ (Fig. 2) and the capacitance per unit length $(C_{e,m})$ (Fig. 3). These effects on the circuit parameters are reflected on the other important parameters of the structure, namely, the characteristics impedance $(Z_{e,m})$ (Fig. 4) and the axial propagation constant (β_m) (Fig. 5). The results presented here are for the first space-harmonic, that is, $m = \pm 1$ including the fundamental mode, which are relevant to the amplification in a TWT or to the prevention of unwanted backward-wave oscillation therein. The structure parameters which have been found significantly influencing the results are the inhomogeneity of the structure and the proximity of the envelope with respect to the helix.

It is found from the Figs. 2a, 3a, 4a, and 5a, the inhomogeneity factor $\chi\ (= \varepsilon'_{r,p}/\varepsilon'_{r,p-1};\ p \leq 3 \leq n+2)$ significantly affects the structure parameters. The value of the inhomogeneity factor $\chi < 1$ and > 1 corresponds to the effective relative permittivities of the equivalent dielectric tube regions decreasing or increasing radially outward from the helix, respectively. The values predicted by the present approach for the first positive space harmonic $(m = +1)$ in respect of $L_{e,m}$, $Z_{e,m}$ increase and of $C_{e,m}$ decreases at faster rate, respectively, and for the first negative space harmonic $(m = -1)$ the value of $L_{e,m}$ decreases and values of $Z_{e,m}$ and $C_{e,m}$ increase as expected. The values of the structured parameters obtained by this present approach for the space-harmonic modes $(m = -1$ and or $+1)$ increases or decreases depending upon $\chi < 1$ or > 1. The metal envelope to helix separation (b/a), also significantly affects these line parameters corresponding to $m = +1$ and $m = -1$. As the envelope is brought closer to the helix i.e. with the decreases in the value of b/a, or with the increase of

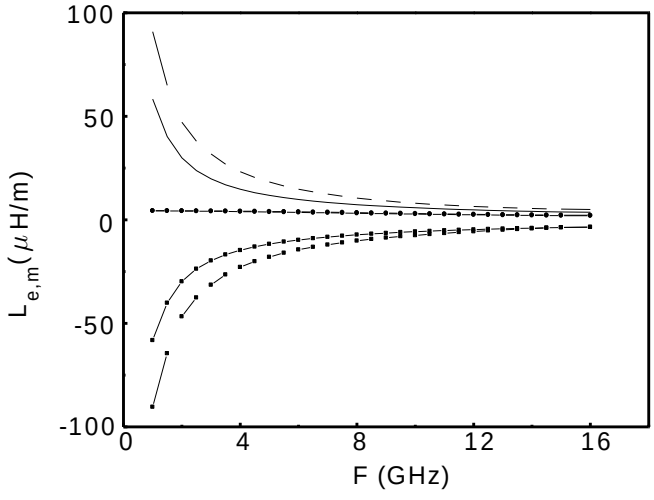

(a)

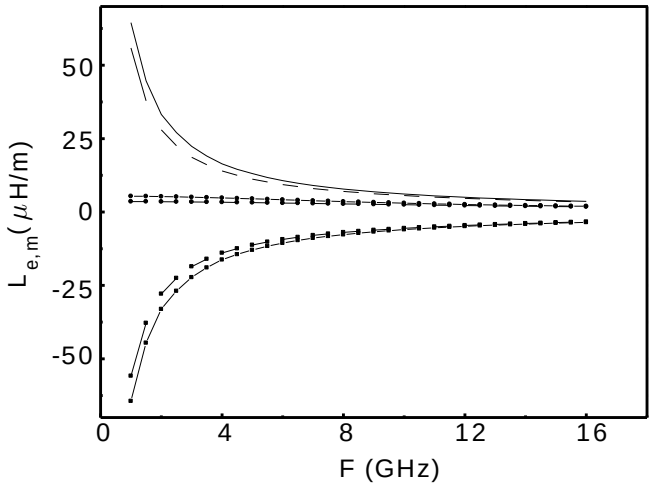

(b)

Figure 2. Frequency response of equivalent series inductance per unit length ($L_{e,m}$) of an inhomogeneously dielectric loaded helix in a metal envelope, taking (a) χ (solid line for 0.9 and broken line for 1.1) ($a = 0.825\,\text{mm},\ b_0 = a,\ \varepsilon'_{r,3} = 2.0,\ b/a = 1.75,\ \cot\psi = 0.8,$ tape width-to-pitch ratio $= 0.50,\ n = 10$), and (b) b/a (solid line for 1.5 and broken line for 2.5) ($a = 0.825\,\text{mm},\ b_0 = a,\ \varepsilon'_{r,3} = 2.0,\ \chi = 1.1,\ \cot\psi = 8.0,$ tape width-to-pitch ratio $= 0.50,\ n = 10$) as the parameters (Line with squares for $m = -1$, line with circles for $m = 0$, and solid lines for $m = +1$).

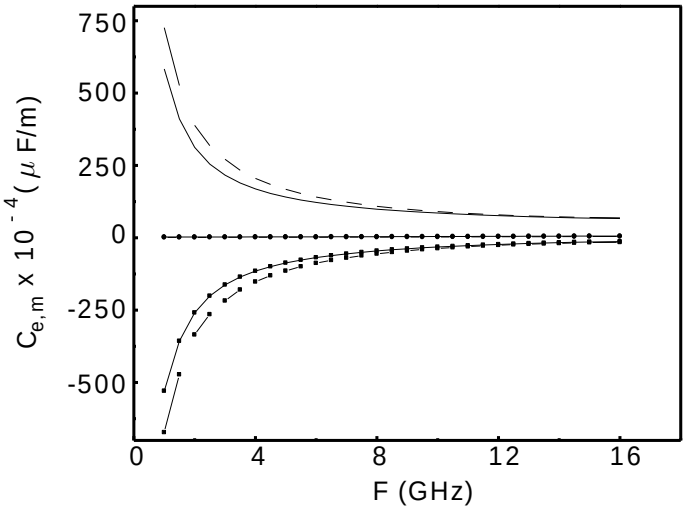

(a)

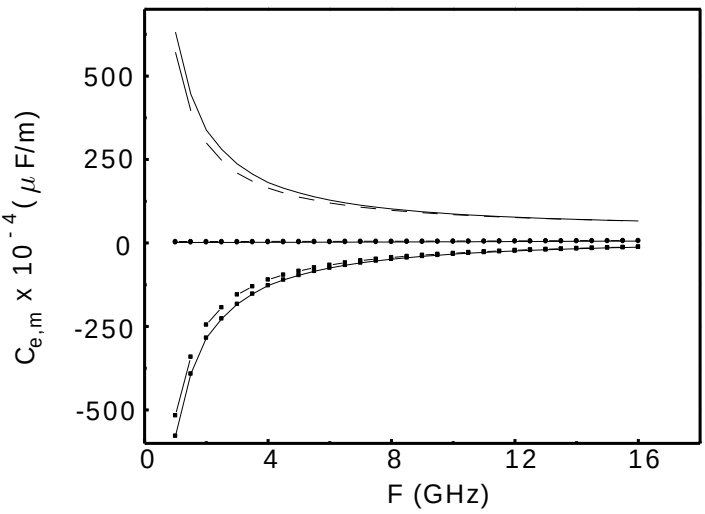

(b)

Figure 3. Frequency response of equivalent shunt capacitance per unit length $(C_{e,m})$, taking (a) χ, and (b) b/a as the parameters, for identical situations as given in Fig. 2.

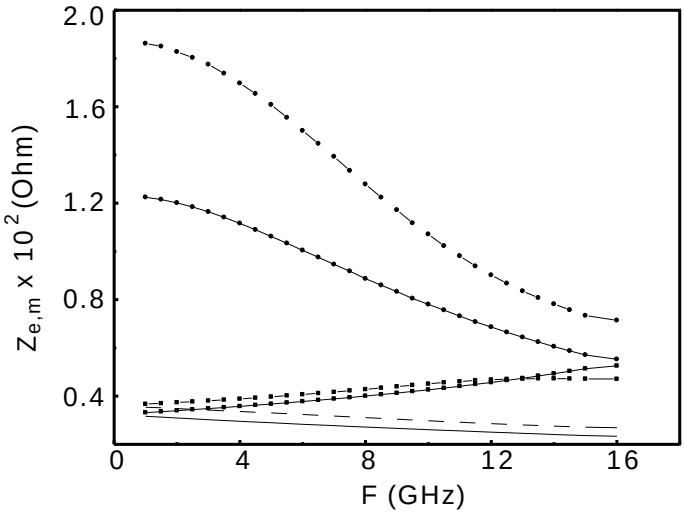

(a)

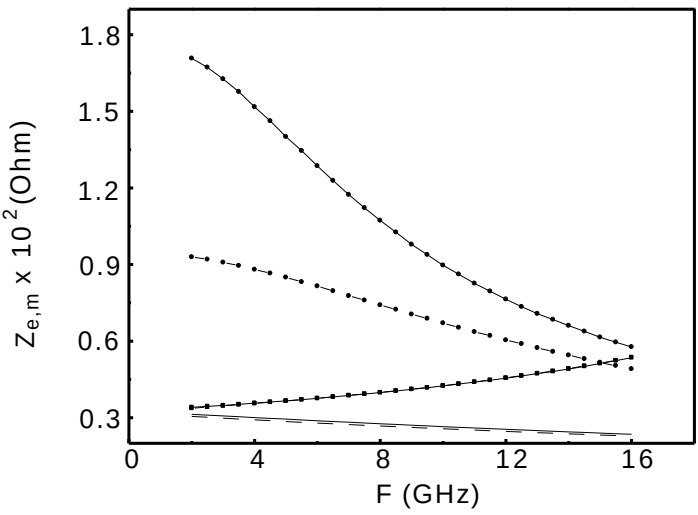

(b)

Figure 4. Frequency response of characteristics impedance $(Z_{e,m})$, taking (a) χ, and (b) b/a as the parameters, for identical situations as given in Fig. 2.

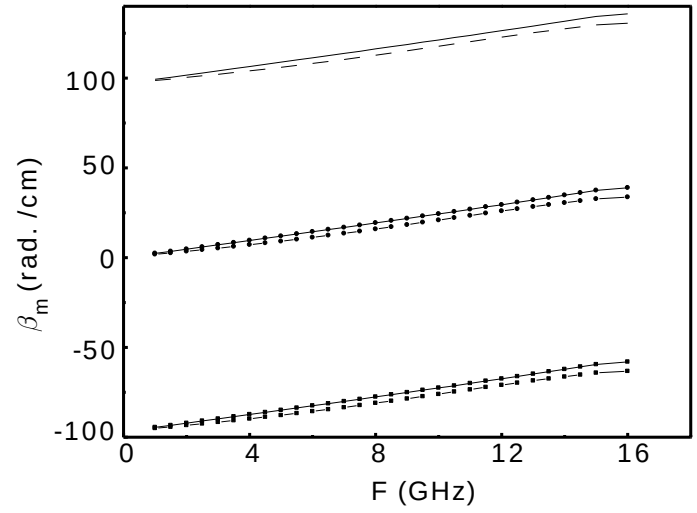

(a)

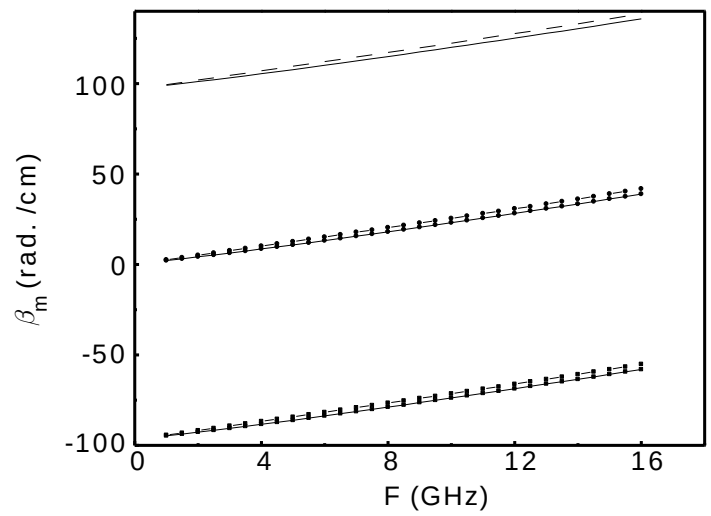

(b)

Figure 5. Frequency response of axial propagation constant ($\beta_{e,m}$), taking (a) χ, and (b) b/a as the parameters, for identical situations as given in Fig. 2.

helix loading the value of $L_{e,m}$ and β_m increases for $m = +1$ and decreases for $C_{e,m}$ and $Z_{e,m}$ However, for $m = 0$ or -1, these effects are reversed. It is found in general that for both the approaches, $L_{e,m}$ and $Z_{e,m}$ decrease with frequency for $m = +1$ and $m = 0$ and $C_{e,m}$ decreases for $m = +1$ and increases for $m = 0$. However, the effect of $m = -1$ on the parameters is reversed. This is due to the decrease of $\beta_m a$ or $\gamma_m a$ for $m = -1$ which will not compensate the increase in $\beta_m a$ or $\gamma_m a$ for $m = +1$ and hence the effects are reversed for $m = -1$.

Experimental Validation

It is worth validating the present analysis with those experimental results for the axial propagation constant of the fundamental mode (zeroth order), reported elsewhere. The results predicted by the present analysis for the fundamental mode $(m = 0)$ of the axial propagation constant β_0, closely agree with those obtained from [15] (Fig. 6). The axial propagation constant β_0 has been obtained by changing the phase velocity v_p $(= \omega/\beta_0)$. For validation of the present theory with experimental results, practical structures, namely, rectangular bar and circular rod supports has been considered. Moreover, helix thickness has also been considered (Fig. 6).

4. CONCLUSION

The present simple and elegant analysis of a helical structure includes the space harmonics considering axial periodicity of the sheath helix [12], the finite helix thickness [13, 14], the structure inhomogeneity for the dielectric supports deviating from the simple wedge geometry [4] from and the non-uniformity of radial propagation constant over the structure cross section. This makes the present analysis more general and capable of dealing with a wide range of structure parameters. This analysis shows its potential to suppress unwanted space-harmonic modes in high voltage and millimeter-wave TWTs or to design space-harmonic devices. Though the results presented here are for the first space-harmonic mode only, it can be evaluated for any mode of space-harmonic of interest. In fact, the results converges for $m \sim \pm 3$ or ± 4. Importantly, the present analysis gives the method of evaluating the transmission line parameters for the mth mode of a sheath model for a dielectric-loaded metal envelope structure in a practical configuration for helix TWTs.

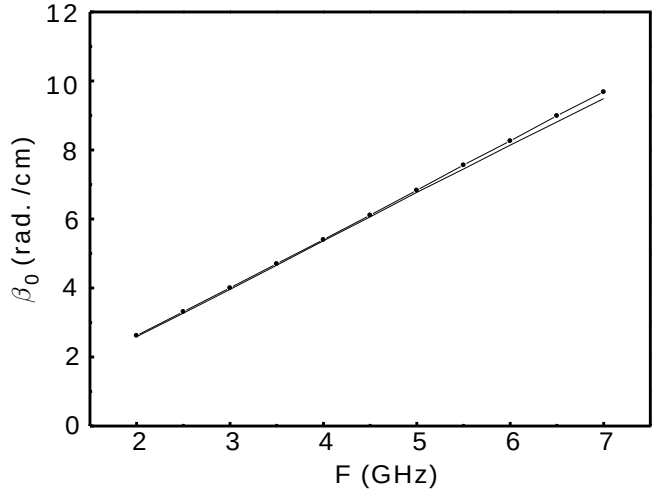

(a)

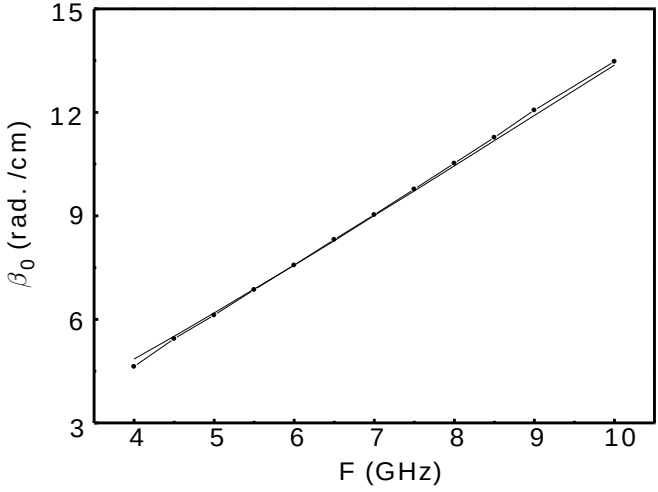

(b)

Figure 6. Comparison between the theoretical (solid line) and experimental (line with circles) [15] values of fundamental mode of axial propagation constant (zeroth order) considering typical structure dimensions including helix thickness $(s = (b_0 - a))$. (a) $a = 2.95\,\text{mm}$, $s = 0.138\,\text{mm}$, $b = 5.13\,\text{mm}$, pitch angle $= 10.12^\circ$, tape width $= 1.27$, $\varepsilon_r = 1.0$, $n = 15$, (b) $a = 1.465\,\text{mm}$, $s = 0.125\,\text{mm}$, $b = 2.92\,\text{mm}$, pitchangle $= 9.50^\circ$, tape width $= 0.89$, $\varepsilon_r = 5.2$, number of supports $= 3$, $n = 15$.

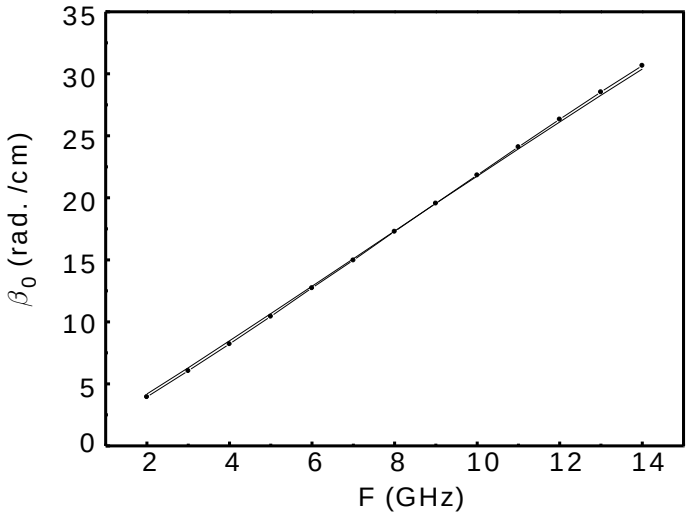

(c)

Figure 6. (c) $a = 0.826\,\text{mm},\ s = 0.063\,\text{mm},\ b = 1.449\,\text{mm},$ pitch angle $= 6.4°,$ tape width $= 0.127,\ \varepsilon_r = 9.0,\ n = 15)$.

APPENDIX A

With the help of $(4n + 6)$ boundary conditions and field expressions one can express the axial electric field (E_z) and the azimuthal electric field (E_θ) intensities at the sheath helix radius $(r = a)$ in terms of the axial and the azimuthal components of sheath helix current, respectively, as:

$$E_{za} = P_c I_{za}, \tag{A.1}$$

$$E_{\theta a} = Q_c I_{\theta a}, \tag{A.2}$$

where

$$P_c = \left(\frac{j\gamma_m^2}{2\pi\omega\varepsilon_0}\right)\left(1 - \frac{m\beta_m \cot\psi}{\gamma_m^2 a}\right)\left(1 - \frac{P_0 I_m\{\gamma_m a\}}{Q_0 K_m\{\gamma_m a\}}\right) I_m\{\gamma_m a\} K_m\{\gamma_m a\}, \tag{A.3}$$

and

$$Q_c = \left(\frac{j\omega\mu_0}{2\pi}\right)\left(1 - \frac{m\beta_m \cot\psi}{\gamma_m^2 a}\right)^{-1}\left(1 + \frac{S_0 I'_m\{\gamma_m a\}}{R_0 K'_m\{\gamma_m a\}}\right) I'_m\{\gamma_m a\} K'_m\{\gamma_m a\}. \tag{A.4}$$

These electric field intensities (A.1) and (A.2) are expressed in terms of circuit potential V and vector potential $\mathbf{A}$ as follows:

$$E_{(z,\theta)a} = -(\nabla V)_{(z,\theta)} - \frac{\partial A_{(z,\theta)}}{\partial t}, \tag{A.5}$$

suffix (z, θ) representing axial (z) and or azimuthal (θ) components.

In the cylindrical coordinate system (A.5) can be written as:

$$E_{(z,\theta)a} = -\frac{\partial V}{\partial(z,\theta)} - \frac{\partial A_{(z,\theta)}}{\partial t}, \tag{A.6}$$

assuming that the rf quantities vary as exp $j(\omega t - \beta_m z - m\theta)$, one may express (A.6) as:

$$E_{za} = j(\beta_m V - \omega A_z), \tag{A.7}$$

$$E_{\theta a} = -j(mV + \omega A_\theta). \tag{A.8}$$

Further, the vector potential $\mathbf{A}$ and the scalar potential V are related through

$$\vec{\nabla} \cdot \vec{A} + \mu_0 \varepsilon_0 \frac{\partial V}{\partial t} = 0, \tag{A.9}$$

expanding (A.9) in the cylindrical coordinate system, and since there is no sheath helix current in the radial direction, i.e., $A_r = 0$, one may express (A.9) as:

$$jmA_\theta/a - \beta_m A_z + \omega \varepsilon_0 \mu_0 V = 0. \tag{A.10}$$

With the help of boundary condition $(E_{za} + E_{\theta a} \cot\psi = 0)$ at the sheath helix, $r = a$, and using (A.7) and (A.8) one may express the azimuthal component of the vector potential A_θ in terms of scalar potential and axial component of the vector potential A_z as:

$$A_\theta = \frac{(\beta_m - m\cot\psi)V - \omega A_z}{\omega \cot\psi}. \tag{A.11}$$

Substituting (A.11) in (A.10) and then in (A.7) one can express E_{za} in terms of circuit potential as:

$$E_{za} = jV \left[\frac{m + a\beta_m \cot\psi}{(\gamma_m^2 a + m^2)\cot\psi} \right]^{-1}, \tag{A.12}$$

with the help of $(A.12)$ and $(A.1)$, the axial component of the sheath helix current expressed in terms of circuit potential V as:

$$I_{za} = j\left(\frac{V}{P_c}\right)\left[\frac{m + a\beta_m \cot\psi}{(\gamma_m^2 a + m^2)\cot\psi}\right]^{-1}. \tag{A.13}$$

Similarly, the expression for the azimuthal component of sheath helix current can be written as:

$$I_{\theta a} = -j\left(\frac{V\tan\psi}{Q_c}\right)\left[\frac{m + a\beta_m \cot\psi}{(\gamma_m^2 a + m^2)\cot\psi}\right]. \tag{A.14}$$

Finally, with the help of telegraphist equation (for a loss less structure), (A.13) and (A.12) and also with the help of the boundary condition $I_{\theta a}\sin\psi = I_{za}\cos\psi$ and after a lengthy algebraic formulations one can get the expressions for shunt capacitance per unit length and series inductance per unit length as:

$$C_{em} = C_{0m}\alpha_{cm}, \tag{A.15}$$

$$L_{em} = L_{0m}\alpha_{1m}. \tag{A.16}$$

ACKNOWLEDGEMENT

Authors are thankful to the Director, CEERI, Pilani for his kind permission to publish this work. They are also thankful to the colleagues of this group for their co-operation to complete this work.

REFERENCES

1. Jain, P. K. and B. N. Basu, "The inhomogeneous loading effects of practical dielectric supports for the helical-slow wave structure of a TWT," *IEEE Trans. on Electron Devices,* Vol. ED-34, 2643–2648, 1987.
2. Ghosh, S., P. K. Jain, and B. N. Basu, "Rigorous tape analysis of inhomogeneously loaded helical slow-wave structures," *IEEE Trans. on Electron Devices,* Vol. ED-44, No. 7, 1158–1168, 1997.
3. Basu, B. N. and A. K. Sinha, "Dispersion-shaping using an inhomogeneous dielectric support for the helix in a travelling-wave tube," *International Journal of Electronics,* Vol. 50, 235–238, 1981.

4. Ghosh, S., P. K. Jain, and B. N. Basu, "Modified field analysis of inhomogeneously-loaded helical slow-wave structures for TWT's," *International Journal of Electronics,* Vol. 81, No. 1, 101–112, 1996.
5. Sinha, A. K., R. Verma, R. K. Gupta, L. Kumar, S. N. Joshi, P. K. Jain, and B. N. Basu, "Simplified tape model of arbitrarily-loaded helical slow-wave structures of a traveling-wave tube," *Proc. IEE, pt-H,* Vol. 139, 347–350, 1992.
6. Ghosh, S., "Analytical studies on inhomogeneously loaded helical structures for broadband TWT's," Ph.D. dissertation, Dept. Electron. Eng., Banaras Hindu Univ., Varanasi, India, 1996.
7. Basu, B. N., "Equivalent circuit analysis of a dielectric-supported helix in a metal shell," *Int. J. Electronics,* Vol. 47, 311–314, 1979.
8. Sinha, A. K. and B. N. Basu, "Circuit parameters for a complex helical SWS combining results for simpler configuration," *Indian J. Pure & Appl. Phy.,* Vol. 50, 235–238, 1980.
9. Kumar, L., R. S. Raju, S. N. Joshi, and B. N. Basu, "Modeling of vane-loaded slow- wave structure for broadband traveling-wave tubes," *IEEE Trans. Electron Devices,* Vol. ED-39, 1961–1965, 1992.
10. Sinha, A. K., R. Verma, Mradula, M. Kundu, R. K. Gupta, and H. N. Bandopadhyay, "Interaction structure for Gyrotrons: A study on dispersion, efficiency and cold design," *Proc. of the Workshop on Gyrotron and Other Fast Wave Devices,* GYROFAD-92, CEERI, Pilani, 1992.
11. Watkins, D. A., *Topics in Electromagnetic Theory,* John Wiley, New York, 1958.
12. Sensiper, S., "Electromagnetic wave propagation on helical structures," *Proc. IRE*, Vol. 43, 149–161, 1955.
13. Ghosh, S., P. K. Jain, and B. N. Basu, "Role of helix thickness in the field analysis and characterisation of the slow-wave structure of a broadband TWT," *J. Inst. Electron & Telecomn. Engrs. of India,* Vol. 14, No. 6, 431–438, 1997.
14. Jain, P. K., K. V. R. Murty, S. N. Joshi, and B. N. Basu, "Effect of the finite thickness of the helix wire on the characteristics of the helical slow-wave structure of a travelling-wave tubes," *IEEE Trans. Electron Devices,* Vol. ED-34, 1209–1213, 1987.
15. D'Agostino, S., F. Emma, and C. Paoloni, "Accurate analysis of helical slow-wave structures," *IEEE Trans. Electron Devices,* Vol. ED-45, 1605–1613, 1998.